SUPPLEMENTAL MATERIAL

EXPANDED MATERIALS & METHODS

Computational Model - Parameter Estimations
Gene expression analysis on cell culture of HAECs perturbed by BMP9 and BMP4 provide estimations for many of the production rates of some chemicals in the mathematical model.

Production Rates

- BMP9 production $\mathbf{k_A}$ was set = 0 to reflect the fact that BMP9 was added exogenously at the beginning and not afterward. The initial condition for A = BMP9 was set to 10, while all other initial conditions were set to 1.

- BMP4 max production rate $\mathbf{k_B}$ = .015 In the supplement to our 2004 PNAS article (40), we said "In additional unpublished findings, we assessed the production of BMP-2 in calcifying vascular cells and in endothelial cells. Rates were ≈ 0.06-0.12 ng/hr for both cell types." This translates to an upper estimate of .12/8 = .015 ng/ml/hr

- Endoglin max production rate ($\mathbf{k_E}$). Estimated to be similar to BMP4 = .015 ng/ml/hr

- ALK1 max production rate ($\mathbf{k_S}$) = 0.75

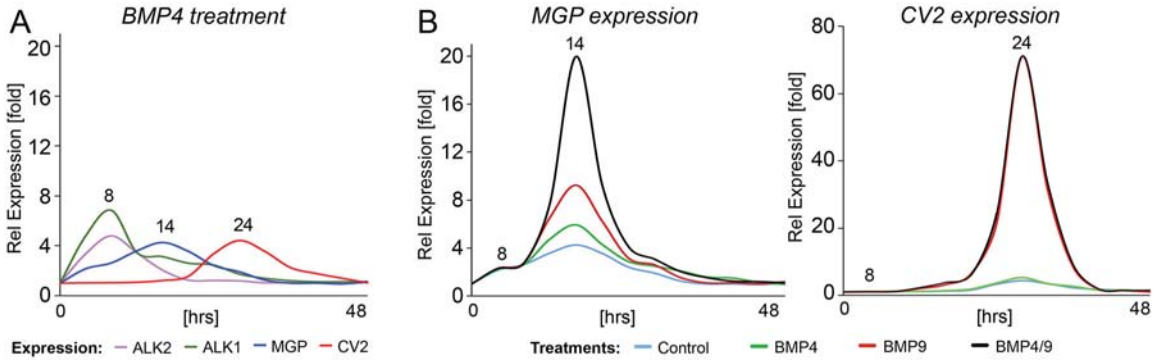

Estimation of ALK1 production time delays and ALK1 production rate with BMP4 treatment (data from Yao et al., 2012 (21))
We assume the initial concentration of ALK1 in the HAEC cell culture system is very low, close to 1 ng/ml. Based on these numbers, the production rate of ALK1 is
k_S = ((7 fold − 1fold) · 1ng/ml) ÷ 8 hrs·
=0.75 ng ml^{-1} hr^{-1}

- MGP max production rate ($\mathbf{k_M}$) (3 ng/ml/hr). Based on the same reasoning, the graph from (Yao et al., 2012 (21)) indicates a rate of ((20 fold-2 fold) · 1 ng/ml) ÷ 14 hrs – 8 hrs = 3 ng ml^{-1} hr^{-1}

- CV2 max production rate ($\mathbf{k_C}$).
k_C =(70 fold – 4 fold) · 1ng/ml ÷ (24hrs − 8hrs)
k_C =4.1 ng · ml · hr

Binding rates

- Binding rate of BMP9 and CV2 (θ_{AC}) = 0.5 (estimate)

- Binding rate of BMP4 and MGP (θ_{BM}) = 0.1 (estimate)

Degradation Rates
In Garfinkel et al. (40), we wrote: "Entchev et al. (5) estimated the upper limit of proteolytic degradation of the BMP-2 homologue, Dpp, as 5% of production rate." Therefore, for each of the proteins, we conservatively estimated proteolytic degradation rates as 3% of the respective production rates.

However, ALK1 elimination occurs primarily through endocytosis from the plasma membrane. Experimental studies have demonstrated that this rate is approximately 1.5 hr^{-1}, which is the value assigned to μ_S (62). BMP turnover is thought to occur primarily through BMP-bound receptor endocytosis, since no extracellular proteases targeting ligands of the TGFβ superfamily have been identified. As a result, the degradation rates of BMP4 and BMP9, μ_A and μ_B respectively, should be within several multiples of μ_S.

- BMP9 degradation μ_A **= 0.5** (based on BMP4)
- BMP4 degradation μ_B **= 0.5** (see text above)
- Endoglin degradation μ_E **= 0.05**
- ALK1 degradation μ_S **= 1.5** (see text above)
- MGP degradation μ_M **= 0.09**
- CV2 degradation μ_C **= 0.12**

Other parameters
- p = $\sqrt{0.1} = 0.31$ estimated
- q = $\sqrt{2} = 1.4$ estimated

Time delays

τ_{ALK1} **=** 2 hrs (based on graph above from Yao et al. 2012 (21))
For example, ALK1 expression dramatically increases after treating HAECs with BMP4, beginning an hour after BMP4 treatment and peaking at 8 hours [1]

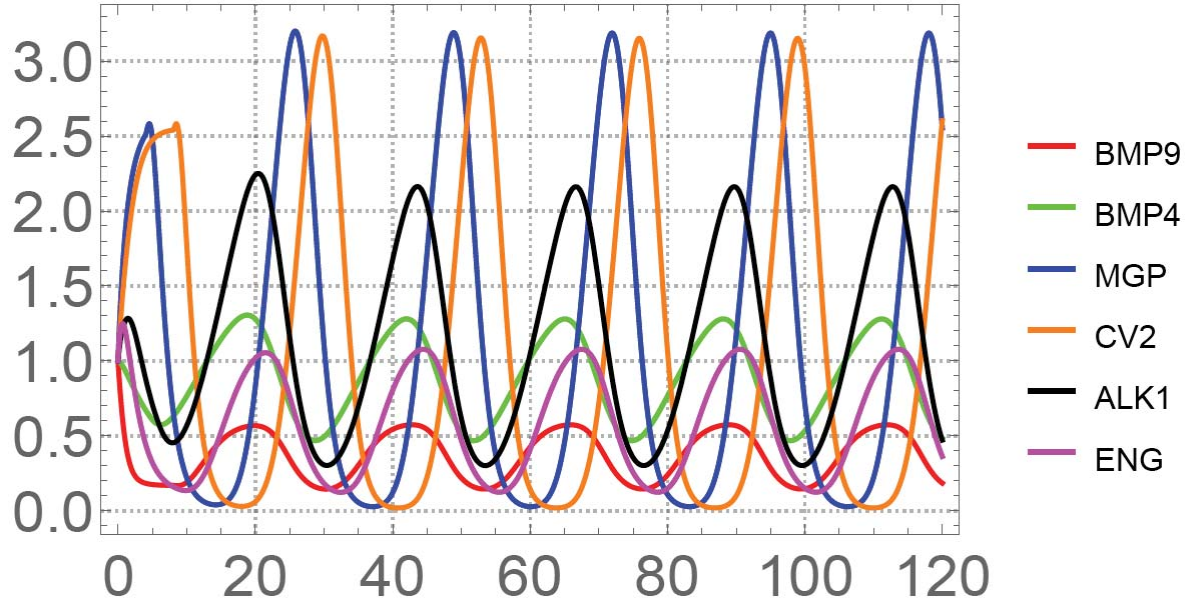

Sample output from the model, using parameters for HAEC-lo (τ_{CV2} = 12, τ_{MGP} = 30)

Mgp-KI Mouse

A *Mgp*$^{mut/mut}$ (*Mgp*-knockin, *Mgp*-KI) mouse, where mutation of Proline-64 eliminates BMP binding (see (26) for sequence and identification of Proline-64 as an critical BMP-binding residue) was generated by the Transgenic & Chimeric Mouse Facility, Perelman School of Medicine, University of Pennsylvania, by homologous recombination on C57BL/6J background as outlined in the figure below. Proline-64 was replaced by a glycine residue, which was verified by sequencing.

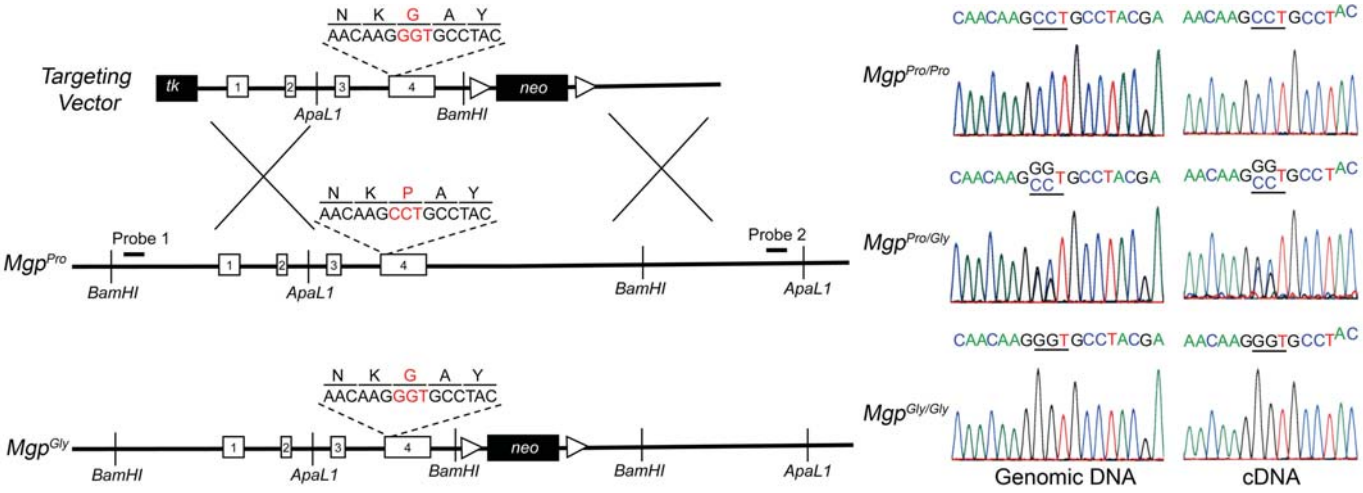

Construction of the Mgp $^{mut/mut}$ *(Mgp-knockin, Mgp-KI) mouse*

(Left) Construction of targeting vector.

(Right) Verification of mutated *Mgp* sequence in the generated *Mgp*-KI mouse.

Retinal Whole Mount Staining

On postnatal day 7, mice eyes were enucleated immediately after euthanasia, retinas were fixed and stained as previously described (50). Briefly, eyes were fixed for 20 min in 4% paraformaldehyde (PFA) at room temperature and transferred to ice cold 2X phosphate-buffered saline (PBS) prior to dissection of the retinas. After retinal isolation, 4 radial incisions were made to flatten the retinas, which were subsequently fixed in -20°C methanol and stored at -20°C prior staining (no more than 3 months). Prior to vascular staining, the samples were washed three times in PBS followed by permeabilization and blockage of nonspecific antibody-binding sites for 60 min in blocking buffer (0.2% bovine serum albumin (BSA), 5% goat serum, and 0.3% Triton X-100 in PBS). Staining was performed with biotinylated Simplicifolia isolectin B4 and/or primary antibodies to alpha smooth muscle actin, CV2, ALK1, MGP, CD31 and Endoglin diluted in blocking buffer overnight at 4°C. *Please see the Major Resource Table in the Supplemental Materials for details on all antibodies.* Isotype IgG control antibodies were used for detection of non-specific staining. These showed no or insignificant staining in the retinas and are not included in the figures.

Prior to addition of secondary antibodies or streptavidin, the samples were washed four times in

0.3% Triton X-100 in PBS, each wash 10 minutes. To detect biotin and/or unconjugated antibodies, Alexa594- or Alexa350-conjugated streptavidin and/or secondary antibodies conjugated to Alexa594 or Alexa488 diluted in wash buffer were added for 4 hours at room temperature, followed by four washes (0.3% Triton X-100 in PBS), each wash 10 minutes. Stained retinas were mounted and examined using a Zeiss Confocal Laser Scanning Microscope (Carl Zeiss, Inc., Thornwood, NY) or an inverted microscope (Eclipse Ti-S; Nikon Instruments Inc., Melville, NY) with digital camera (DS-Fi2; Nikon Instruments Inc.) at room temperature. ImageJ (NIH Image) was used for data analysis and figures were assembled using Adobe® Photoshop® with adjustment for brightness and/or contrast only.

Vascular shunting
Fifteen-μm fluorescent microspheres (Invitrogen) were injected into the left ventricle immediately after sacrificing the mice, and the retinas were examined and photographed under bright field and fluorescent light. Retained beads were counted on the photos.

Cells and Cell Culture
Human pulmonary artery endothelial cells (HPAECs) and low passage human aortic endothelial cells (HAECs-low passage) were provided by Thermo Fisher Scientific, whereas human saphenous vein endothelial cells (HSVEC) were from Promocell. The human brain endothelial cell line HBEC-5i was provided by ATCC®. *Please see the Major Resource Table in the Supplemental Materials for details.*

The HBEC had near undetectable expression of MGP and was used as MGP-deficient cells due to technical difficulties in generating *Mgp*-null ECs for time course experiments. All the cells were maintained as per the providers' recommendations and used between passages 3-5.

Adipose tissue-derived endothelial progenitor cells, referred to as dedifferentiated fat (DFAT) cells, were prepared and cultured as previously described (63) and used between passages 3-5. High passage HAEC (HAEC-high passage) were obtained and cultured as previously described (64) and were used between passages 10-13.

Generally, the medium was changed every other day and the cells were cultured up to five passages, unless otherwise specified. For experiments, the cells were seeded at $2.5x10^3$ cells/cm^2 and cultured in M200 medium supplemented with low serum growth supplement (LSGS) containing 2% FBS, hydrocortisone (1 μg/ml), human epidermal growth factor (10 ng/ml), basic fibroblast growth factor (3 ng/ml) and heparin (10 μg/ml).

RNA analysis
Total RNA was isolated from tissues or cultured cells using the NucleoSpin® RNA (Takara, Mountain View, CA) according to the manufacturer's instructions; cDNA was obtained using the High Capacity cDNA Reverse Transcription kit (Applied Biosystems, Foster City, CA). Relative quantitative PCR was performed on a 7500 Fast Real-Time PCR System using TaqMan® Universal PCR Master Mix (both from Applied Biosystems). Primers and probes for human or mouse genes were obtained from Applied Biosystems as part of Taqman® Gene Expression Assays. *Please see the Major Resource Table in the Supplemental Materials for details.* Cycle conditions were: one cycle at 50°C for two minutes, followed by one cycle at 95°C for ten minutes, followed by 40 cycles at 95°C for 15 seconds and 60°C for one minute. Threshold cycles of specific cDNAs were compared to the housekeeping gene glyceraldehyde-3-phosphate dehydrogenase (GAPDH) and translated to relative values as previously described (65). All reactions were run in triplicates or quadruplicates. For time course experiments, each time point represented the mean of 3 determinations. All samples were then normalized to GAPDH, and the BMP9-treated samples were subsequently normalized to their own controls.

Cell Proliferation
Cell prolferation was determined after 4 days of culture by counting the cells after trypsinization using a Countess™ II Automated Cell Counter (Thermo Fisher Scientific). For time course experiments, however, cell proliferation was determined using the CyQUANT™ cell proliferation assay for cells in culture (Thermo Fisher Scientific), which measures the cellular DNA content. The proliferation was measured for 6 hours periods. The assay was performed as per the manufacturer's protocol.

Immunoblotting
Immunoblotting was performed as previously described (66). Equal amounts of cellular protein were used, after determination using the Pierce™ BCA protein assay kit (Themo Fisher Scientific). The blots were incubated with specific antibodies to CV2, MGP. β-Actin was used as loading control. *Please see the Major Resource Table in the Supplemental Materials for details.*

Analysis of MGP expression endothelial cells from developing lungs
We obtained a publicly available data set (GSE119228) of single cell RNA-sequencing (scRNA-seq) of cells from developing lungs (51). The sequencing data from non-immune cells were analyzed using the R Package Seurat, version 3.1. To identify oscillatory genes from the target cell population, we employed the Oscope algorithm (52) to the gene expression of the endothelial cells in the EC3 cluster.

Statistics and Scientific Rigor
For time course experiments, each time point represented the mean of 3 determinations. All samples were then normalized to GAPDH, and the BMP9-treated samples were subsequently normalized to their own controls. For the resulting time series data, we employed exponential smoothing function in Excel to analyze the time series of gene expression data. We applied the non-linear polynomial regression and used adjusted R^2 to estimate the ratio of the changes in gene expression that can be explained by the time process, which would indicate the presence of variations that occur at specific regular intervals and would be consistent with periodic oscillations in the gene expression. The non-linear polynomial regression was performed in Microsoft Excel® (adopted from (67, 68)).

For two-group comparisons and multiple-group comparisons, we used the non-parametric Mann-Whitney U test Kruskal-Wallis H test, respectively (GraphPad PRISM® Version 6.0c, GraphPad, San Diego CA). Statistical significance was assigned at $p<0.05$. The number of replicate experiments are provided in the figure legends.

The mouse genotyping and the retinal staining were routinely performed by separate researchers in a blinded manner. The time course experiments were performed by one researcher and then examined by at least two other researchers in a blinded fashion.

Validation of Antibodies
The specificity of all antibodies was verified prior to use for immunoblotting and immunostaining as previously described for the ALK1, CV2, and β-actin antibodies (66). The CD31 and Endoglin antibodies were verified using endothelial cells known to express the particular antigen by qPCR and compared to cells with minimal expression of the antigen. The anti-MGP antibodies were validated using tissues from wild type and *Mgp*$^{-/-}$ mice as shown in the figure below.

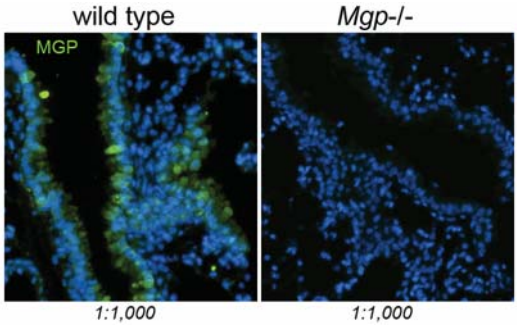

Validation of anti-MGP antibodies (Abcam, AB192396)
The antibodies were tested at dilution 1:1,000 on lung tissue from wild type (left) and *Mgp*-null mice (right). The correct dilution is critical for these antibodies, and depends on the tissue that is stained.

ONLINE FIGURES

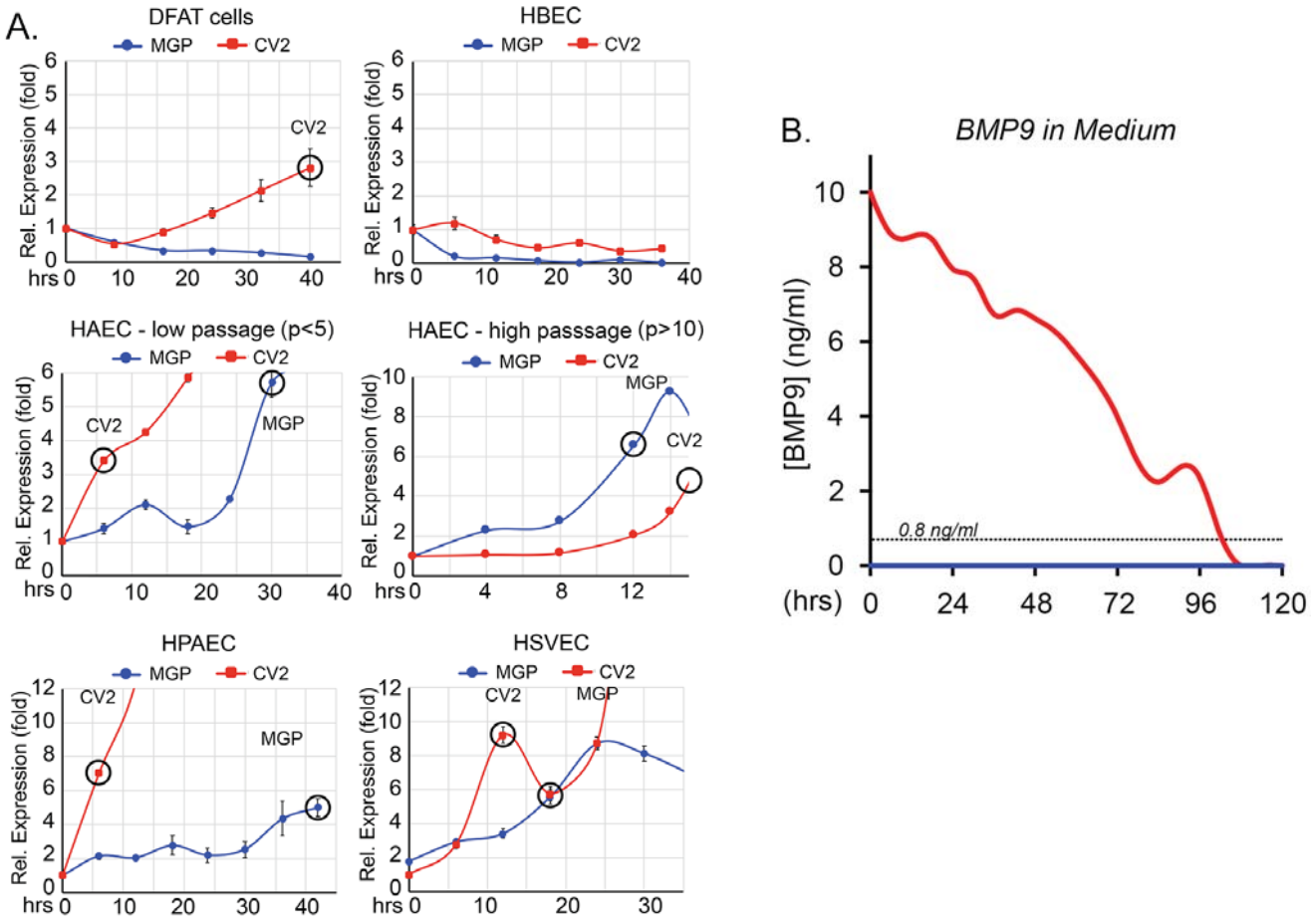

Online Figure I

(A) *Induction of MGP and CV2 in ECs in response to BMP9 (10 ng/ml).*

RNA was collected every 4-8 hours and expression of MGP and CV2 was determined by qPCR. The time of induction (vertical lines) was identified as the time of at least a 3-fold increase in expression of MGP or CV2, as compared to the baseline level at 0 hours (mean±SD of 3 determinations, normalized to GAPDH; 3 replicate experiments were examined).
DFAT cells, dedifferentiated cells; EC, endothelial cells; HPAEC, human pulmonary artery EC; HAEC, human aortic EC; HUVEC, human umbilical vein EC; HBEC, human brain EC; HSVEC, human saphenous vein EC.

(B) *BMP9 concentration in the medium from HPAEC time course experiment.*

Samples were collected from the medium every 6 hours, and the BMP9 concentration was determined by ELISA (duplicate experiments).

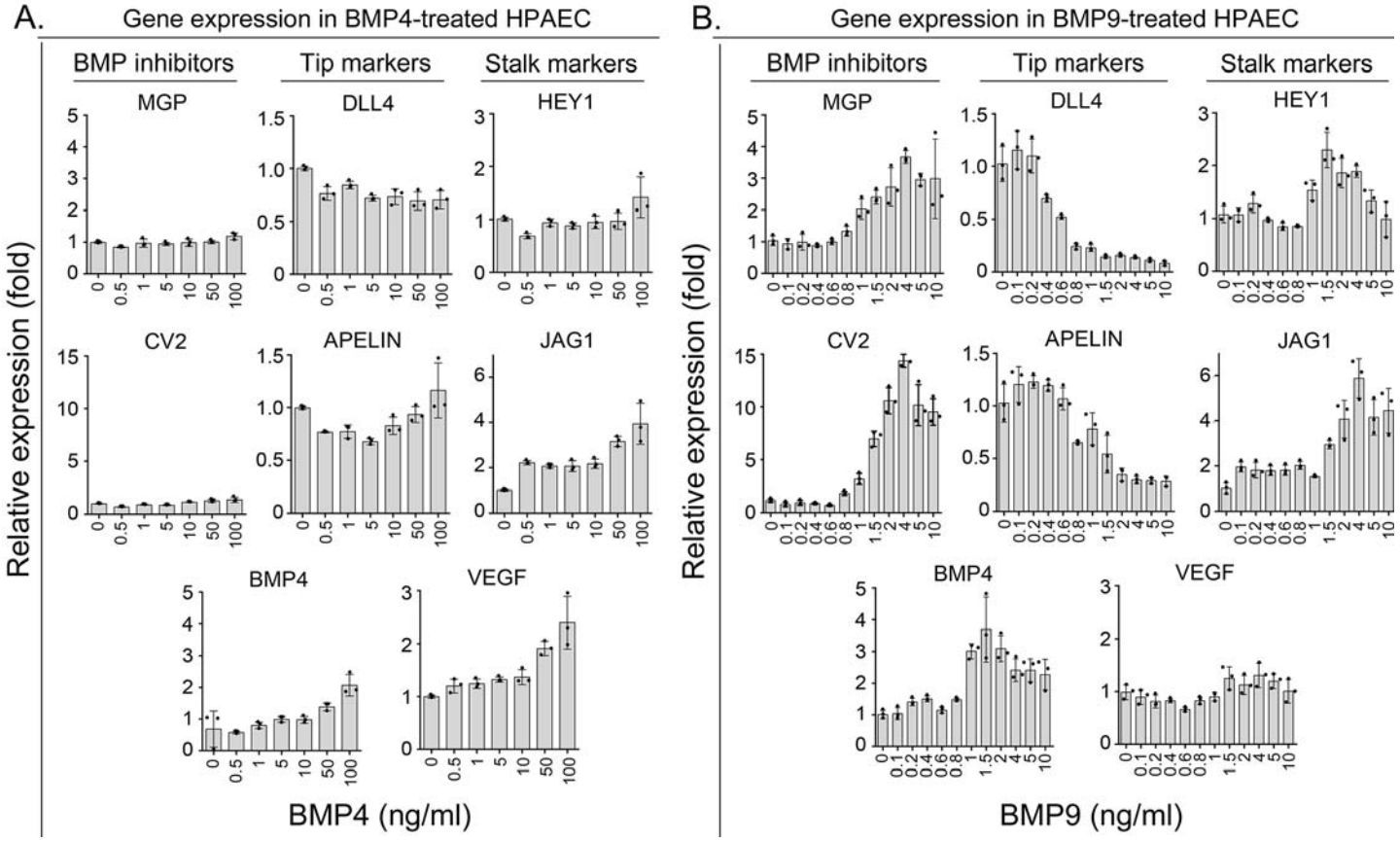

Online Figure II

BMP9 but not BMP4 triggers expression of stalk cell markers in HPAEC

(A, B) To investigate the behavior of tip versus stalk cell markers, we validated that the HPAECs were responsive to BMP4 and BMP9. The cells were treated with increasing concentrations of (A) BMP4 (0-100 ng/ml) or (B) BMP9 (0-10 ng/ml) for 4 days. Expression of BMP inhibitors (MGP and CV2), tip cell markers (Dll4 and Apelin), stalk cell markers (HEY1 and JAG1), and BMP4 was determined by qPCR. BMP4 did not significantly induce expression of any of the transcripts, except for an increase in JAG1 and endogenous BMP4 expression. However, BMP9 induced CV2 and MGP at concentration <1 ng/ml and stalk cell markers at slightly higher concentrations, whereas the expression of tip cell markers was suppressed. This supports that BMP9 promotes the stalk cell phenotype and endothelial maturation (mean+SD of 3 determinations, normalized to GAPDH; representative of 2 or 3 replicated experiments).

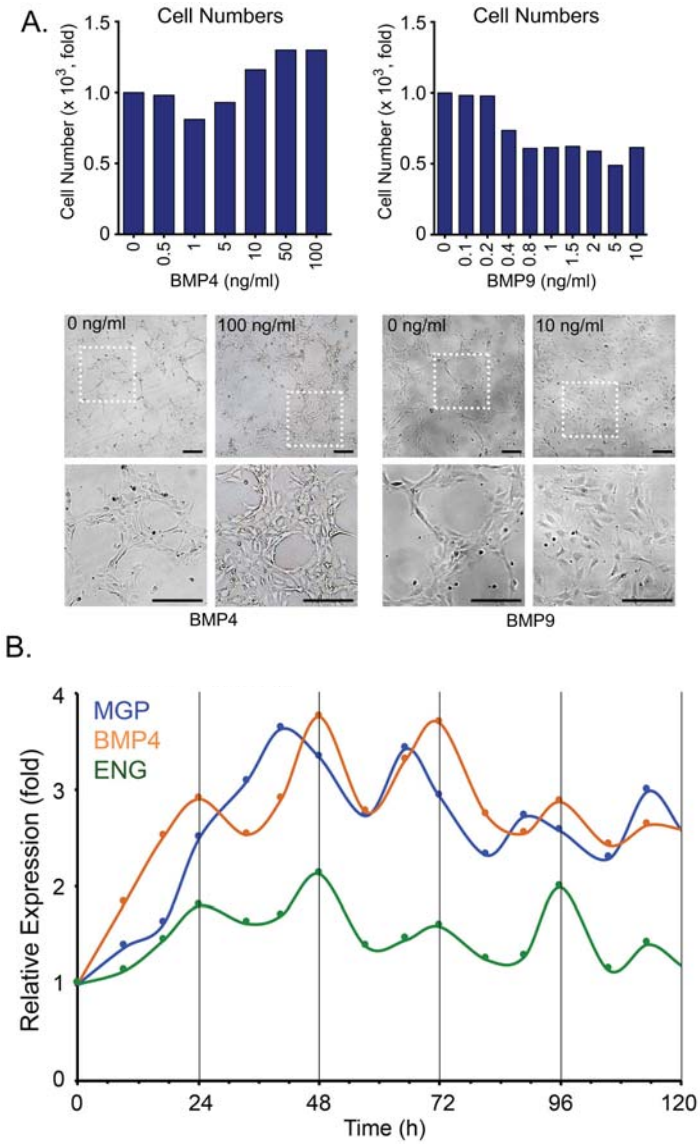

Online Figure III

(A) *Proliferation in HPAECs in response to BMP4 and BMP9.*

We compared the effects of BMP4 and BMP9 on parameters associated with vascular growth including VEGF expression, cell numbers, and growth patterns in the HPAECs.
(**Top panels**) HPAECs were treated with BMP4 (0-100 ng/ml) or BMP9 (0-10 ng/ml) for 4 days when proliferation was determined by cell counting (representative of 3 replicate experiments). The cell numbers increased in response to high concentrations of BMP4 but decreased in response to BMP9. (**Bottom panels**) Images of the HPAECs at the end of the respective treatment. BMP4-treated HPAECs also maintained cellular "strings" in culture, whereas BMP9-treated HAPECs became evenly distributed on the plastic, resembling stalk cell morphology. Thus, BMP4 and BMP9 appear to be associated with a proliferative phase and a maturation phase, respectively. Original magnification was 4X and 10X for the upper and lower images, respectively.

(B) Temporal oscillations in BMP4 in HPAECs

HPAECs were treated with control medium or BMP9 (10 ng/ml), RNA was collected every 8 hours for up to 120 hours, and expression of BMP4 was determined by qPCR, first normalized to GAPDH and then its own control, and compared to MGP and Endoglin (ENG) (duplicate experiments).

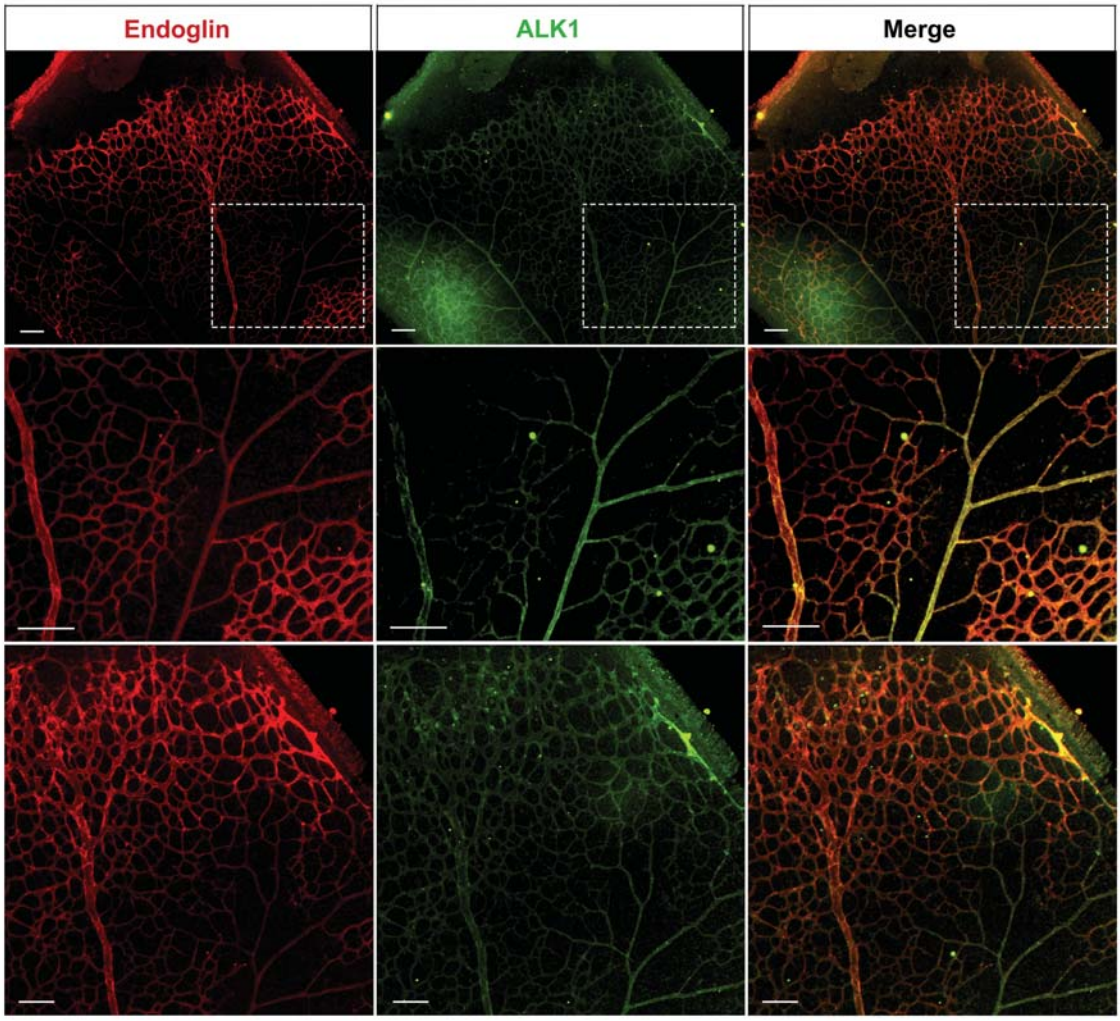

Online Figure IV

Distribution of Endoglin and ALK1 in retinal angiogenesis (postnatal day 7)

Immunofluorescence showing Endoglin staining (red, left panels) together with ALK1 staining (green, middle panels) and merged (right panels). The middle row shows close up of areas indicated in the upper row (bars, 200 µm) (representative of >5 replicate experiments).

The results showed that both ALK1 and Endoglin were detectable in the retina. ALK1 expression was strongest in the retinal arteries, whereas Endoglin expression was most pronounced in the retinal veins and the peripheral collection system.

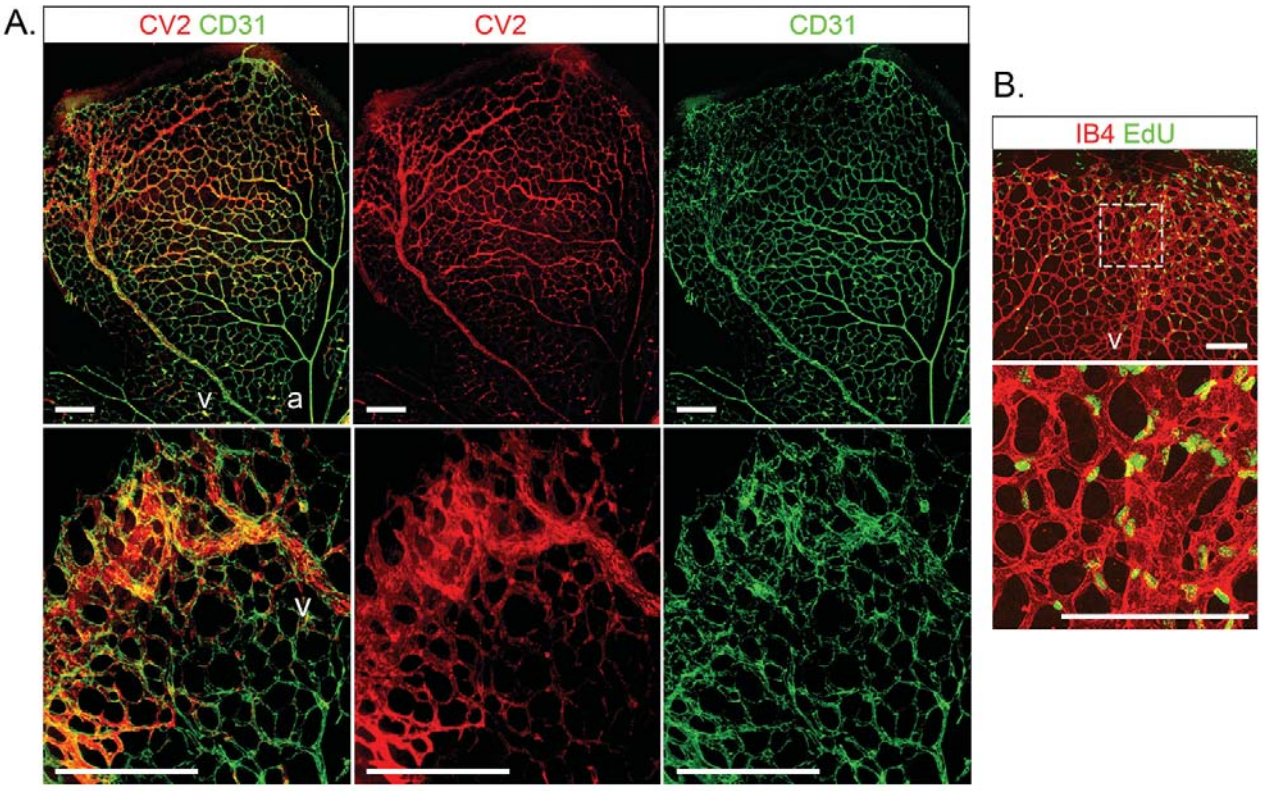

Online Figure V

Distribution of CV2 and CD31 in retinal angiogenesis (postnatal day 7)

(A) (**Top panels**) Immunofluorescence showing the distribution of CV2 staining (red) together with CD31staining (green) in wild type mouse. (**Bottom panels**) Close up of the angiogenic retinal front in proximity of the retinal vein (bars, 200 µm).

(B) EdU staining (green) together with Isolectin B4 (IB4) staining (red) showing proliferation in the venous drainage area of the retinal angiogenic front (bars, 200 µm).

a, artery; v, vein; both panels are representative of >3 replicate experiments.

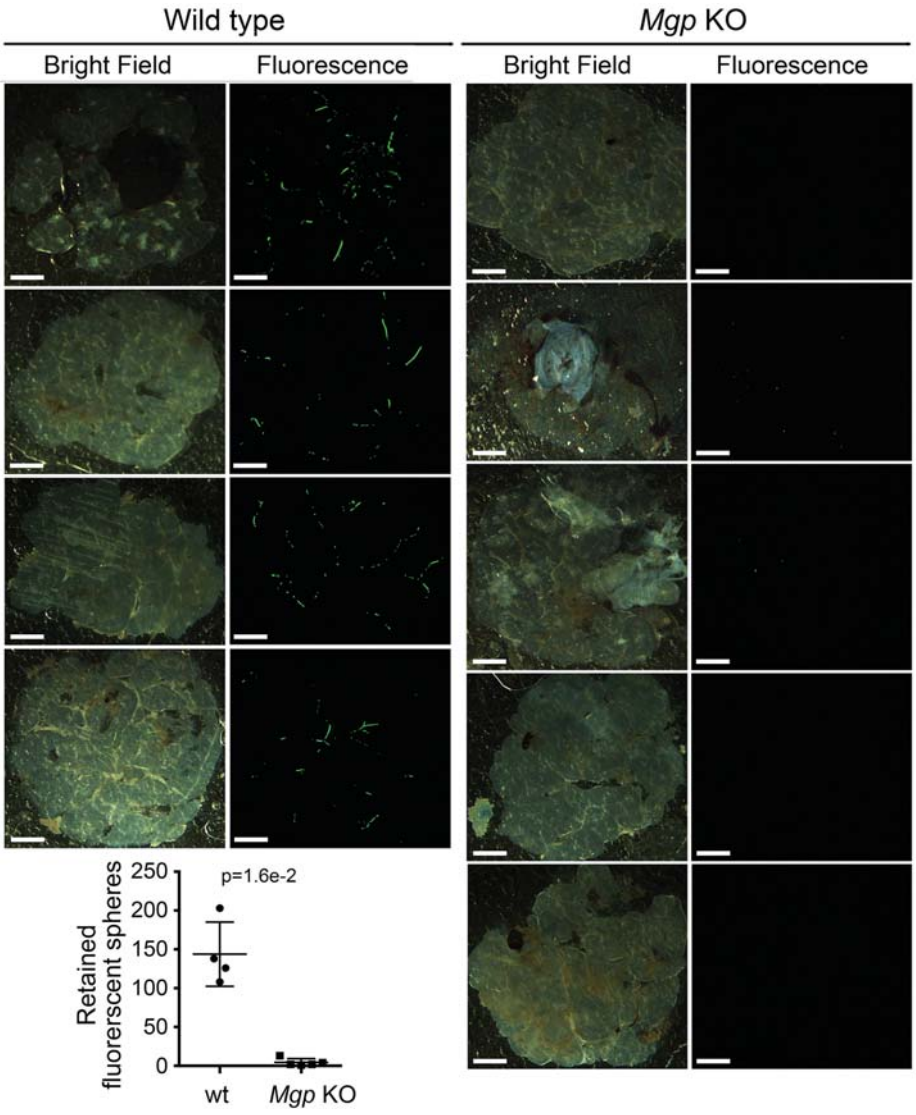

Online Figure VI

Evidence of retinal AVMs

Wild type and Mgp-KO mice were injected with fluorescent microspheres (15 μm) through the left ventricle. The retinas were isolated and visualized under bright field and green fluorescent light (bars, 100 μm). The microspheres in each retina were counted and plotted (mean±SD, n=4-5 retinas, Mann-Whitney test).

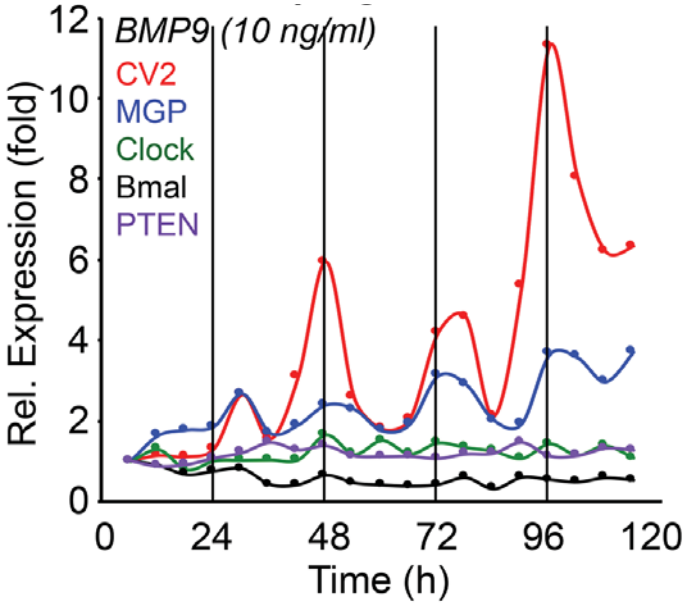

Online Figure VII

Absence of temporal oscillations in Clock, Bmal1 and PTEN in HPAECs

HPAECs were treated with control medium or BMP9 (10 ng/ml), RNA was collected every 6 hours for up to 120 hours, and expression of Clock, Bmal1 and PTEN was determined by qPCR, each time point is the mean of 3 determinations, first normalized to GAPDH and then its own control, and compared to CV2 and MGP (representative of 3 replicate experiments).

CV2, Crossveinless 2; MGP, Matrix Gla protein; Clock and Bmal, clock genes; PTEN, Phosphatase and tensin homolog (PTEN)